Supporting Information for:

Solvent Effects on the Thermal Isomerization Process of a Rotary Molecular Motor

Anouk S. Lubbe, Jos C. M. Kistemaker, Esther J. Smits and Ben L. Feringa*

Center for Systems Chemistry, Stratingh Institute for Chemistry and Zernike Institute for Advanced Materials, University of Groningen, Nijenborgh 4, 9747 AG Groningen, The Netherlands.

b.l.feringa@rug.nl

Contents

1. Application of the modified Eyring equation

In our previous work, a viscosity-corrected form of the Eyring equation was defined:[1]

$$k = \frac{k_B T}{h} e^{-\frac{H_{\eta 1} \ln \eta + H_{\eta 2}}{RT} + \frac{S_{\eta 1} \ln \eta + S_{\eta 2}}{R}} \quad (1)$$

which takes into account the original Eyring equation and Andrade's equation:

$$\ln k = \ln\left(\frac{k_B T}{h}\right) + \frac{S}{R} - \frac{H}{RT} \quad (2)$$

$$\ln \eta = v + \frac{w}{T} \quad (3)$$

and the linear relation between the logarithms of the rate constant k and the viscosity η as predicted by free-volume theory,[2]

$$\ln k = \beta - \alpha \cdot \ln \eta. \quad (4)$$

Here T denotes the temperature, kB is the Boltzmann constant, h is the Planck constant, R represents the universal gas constant, and finally v, w are viscosity parameters and S and H are kinetic parameters of which the values are obtainable from experiment.

In short, equation 2 can be rewritten as follows:

$$\ln k = \ln \frac{k_B T}{h} + \frac{d_1 T^3 + d_2 T^2 + d_3 T + d_4}{c_4 T^3 + c_5 T^2 + c_6 T} + \frac{c_1 T^2 + c_2 T + c_3}{c_4 T^2 + c_5 T + c_6} \cdot \ln \eta \quad (4)$$

Where d_1–d_4 and c_1–c_6 are variables that can be extracted from experimental data.

The viscosity of solvents changes with temperature. The obtained function allows for the creation of a full three dimensional graph of viscosity, temperature and rate. Fitting the linear Eyring equation over isoviscous ranges affords isoviscous kinetic parameters (H_η and S_η) which were found to be linearly dependent on the viscosity.

$$\Delta^{\ddagger} H_\eta = H_{\eta 1} \ln \eta + H_{\eta 2}, \quad (5)$$

$$\Delta^{\ddagger} S_\eta = S_{\eta 1} \ln \eta + S_{\eta 2}, \quad (6)$$

$$\Delta^{\ddagger} G_\eta = H_{\eta 1} \ln \eta + H_{\eta 2} - S_{\eta 1} \ln \eta T - S_{\eta 2} T. \quad (7)$$

This leads to the viscosity-corrected Eyring equation 1.

This method was applied to the isomerization in the methanol/glycol/glycerol series of solvents in order to compare this series with the previously published data for the alkane series of solvents.[1] A direct Eyring plot was constructed for methanol, 40% glycol in methanol and 50% glycerol in methanol (see Section 4). Additionally, the viscosity of these solvent mixtures was measured at 6 different temperatures. Parameters v and w were obtained by plotting ln η against T (Figure 1).

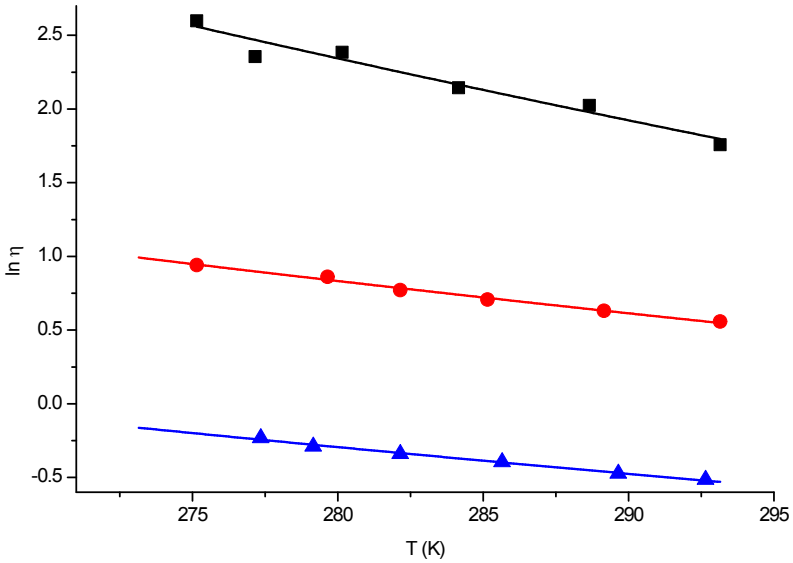

Figure 1: Natural logarithm of viscosity versus temperature for methanol (blue triangles), 40% glycol in methanol (red circles) and 50% glycerol in methanol (black squares), with corresponding fits to obtain parameters *v* and *w*.

The temperature dependent parameters of the viscosity of the solvent and the rate of the isomerization are summarized in Table 1.

Table 1: Temperature dependent parameters of solvent viscosity and activation parameters obtained by direct Eyring analysis.

	MeOH	MeOH 40% Glycol	MeOH 50% Glycerol
v	-5.55±0.23	-5.52±0.30	-9.85±1.70
w	1471±64	1778±86	3415±477
adj. R^2	0.988	0.985	0.894
***η* at rt**	0.589±0.010	1.73±0.05	6.03±1.10
$\Delta^{\ddagger}H^{o}$ (kJ mol^{-1})	79.0±1.4	83.0±2.7	87.4±1.7
$\Delta^{\ddagger}S^{o}$ (J K^{-1} mol^{-1})	-32.0±5.1	-21.7±9.4	-9.9±6.1
adj. R^2	0.999	0.997	0.997
$\Delta^{\ddagger}G^{o}$ (kJ mol^{-1})	88.4±0.1	89.4±0.1	90.3±0.1

Subsequently from these parameters the viables c_1-c_6 and d_1-d_4 were calculated.

Table 2: Calculated parameters

c1	c2	c3	c4	c5	c6	d1	d2	d3	d4
-5.86	$4.83 \cdot 10^3$	$-9.90 \cdot 10^5$	12.4	$-1.03 \cdot 10^4$	$2.18 \cdot 10^6$	9.10	$-1.45 \cdot 10^5$	$1.15 \cdot 10^8$	$-2.40 \cdot 10^{10}$

From these values, the temperature dependent α and R^2 plot of the methanol/glycol/glycerol series was constructed (Figure 2a), and a temperature dependent plot of the β value of both the methanol/glycol/glycerol series and the alkane series (Figure 2b). Over the temperature range under investigation, the alkane series has on average a higher β (~1.3 kJ/mol) than methanol/glycol/glycerol.

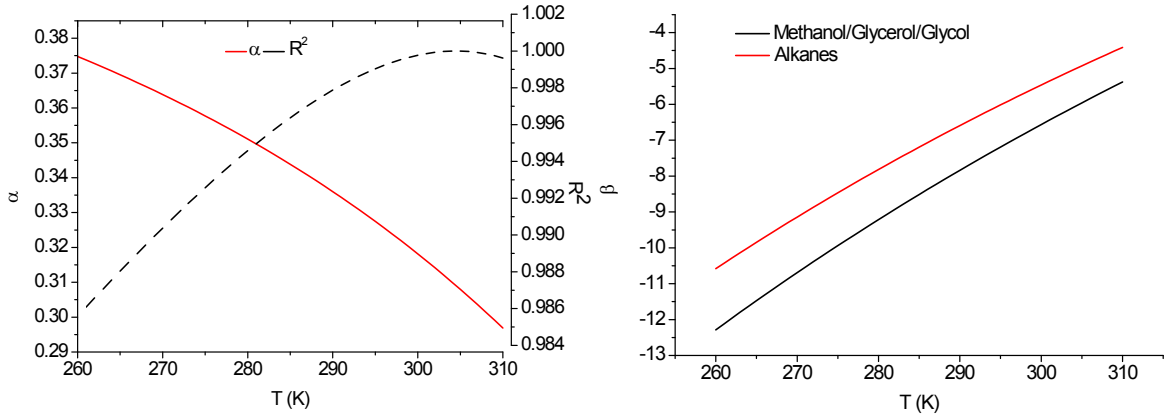

Figure 2: Temperature dependence of parameters for the methanol/glycol/clycerol series: a) α and R^2, b) β.

From the data, by fitting equation 1, the viscosity corrected activation parameters of the methanol/glycol/glycerol series can be obtained, which are shown in Table 3 where they are compared to the previously published viscosity corrected activation parameters of the alkane series.

Table 3: The viscosity corrected activation parameters of both series under investigation.

	$H_{\eta 1}$	$H_{\eta 2}$	$S_{\eta 1}$	$S_{\eta 2}$
Methanol/Glycol/Glycerol	0.86±0.61	76.0±0.5	0.17±2.11	−43.9±1.7
Alkanes	2.71±1.03	77.0±8.0	6.95±3.66	−36.6±2.8

Interestingly, at a viscosity of 1 cP (ln η = 0) the enthalpy of activation ($H_{\eta 2}$) is actually predicted lower for the methanol/glycol/glycerol series than that of the alkane series. However, this is reversed by correcting the barrier of activation with the entropy of activation ($S_{\eta 2}$) which is significantly higher for methanol/glycol/glycerol than for the alkane series. This agrees with the hypothesis that an ordered cage of hydrogen bonds has to be disturbed during the thermal helix inversion, which is expressed in the negative entropy of activation. These conclusions should not be taken without prudence, since the errors on the activation parameters in combination with an enthalpy entropy compensation effect could theoretically shift this balance.[3] However, there is a clear difference in activation energy between the two series which, under the overlapping experimental conditions (n = 0.6 – 2.2 cP, T = 0.0 – 20 °C), averages at 1.1 kJ/mol (ranging from 0.99 – 1.3 kJ/mol). This indicates that on average, it requires the motor to overcome an additional barrier of 1.1 kJ/mol, which is imposed on it by the proposed hydrogen bond cage.

2. Kinetic Experiments.

A $2 \cdot 10^{-5}$ M solution of motor **1** was prepared in the selected solvents. All solvents were purged with argon before use. Samples were prepared in quartz cuvettes (l = 1 cm). The samples were irradiated for 1 h with 365 nm light at −20 °C, 4 °C or 20 °C. The absorption at 410 nm was then measured over time until the relevant band had completely disappeared. A 400 nm cut-off filter was mounted before the light source to minimize photochemistry occurring during the THI. All exponential decay lines were fitted using least squares. Figure 4 shows all recorded exponential decay lines in methanol, as a typical example.

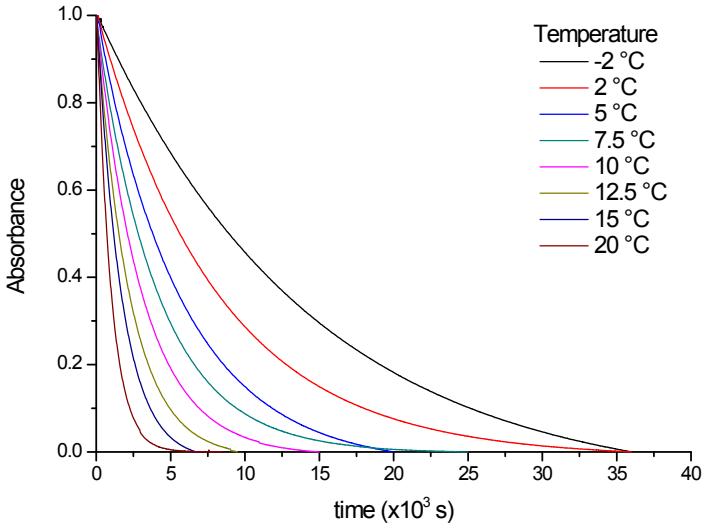

Figure 3: Normalized exponential decay lines from metastable-**1** to stable-**1** in methanol. Absorbance measured over time at 410 nm.

Subsequently, the results were processed using a direct Eyring analysis with errors obtained by a Monte Carlo experiment. Figure 5 shows the Eyring plots for 18 solvents.

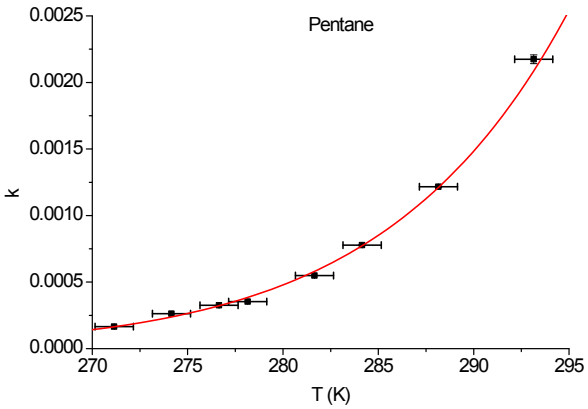
Pentane
k
T (K)

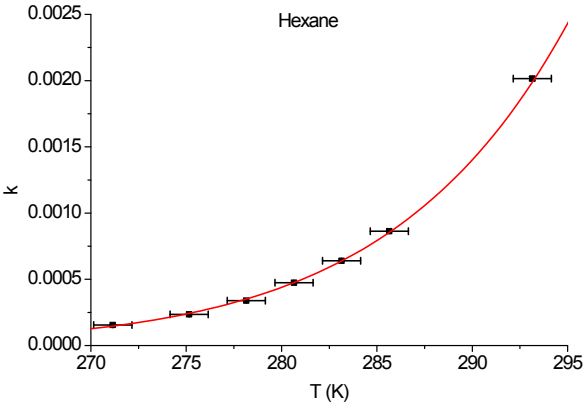
Hexane
k
T (K)

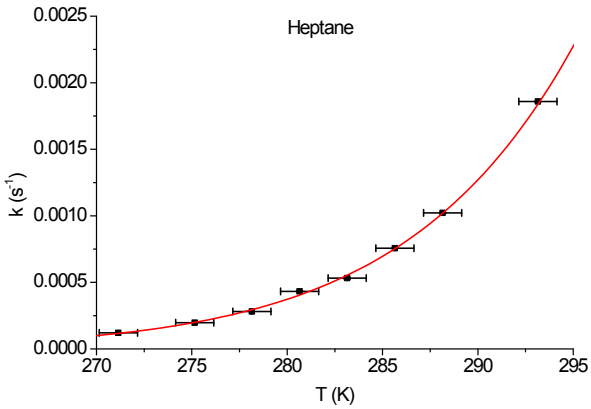
Heptane
k (s-1)
T (K)

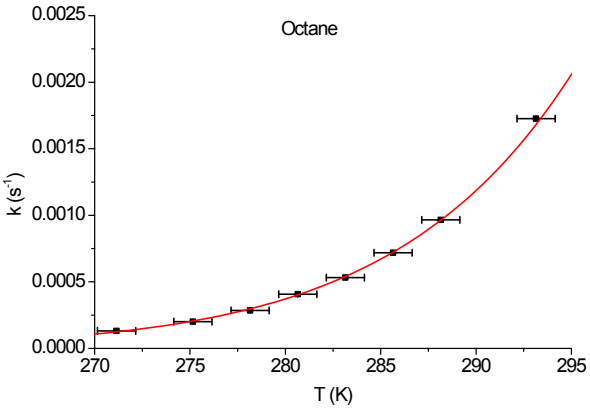
Octane
k (s-1)
T (K)

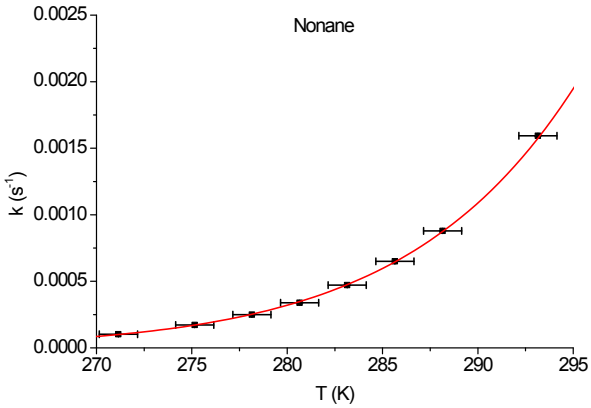
Nonane
k (s-1)
T (K)

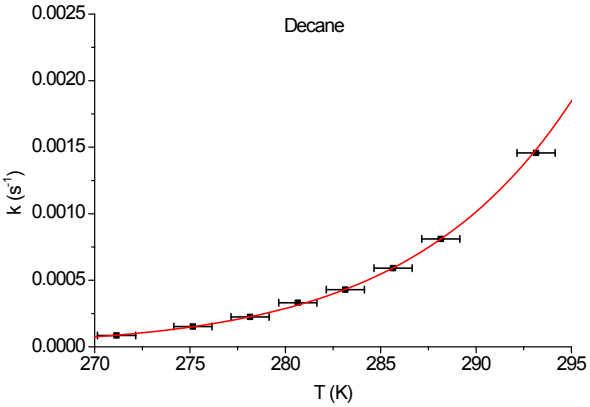
Decane
k (s-1)
T (K)

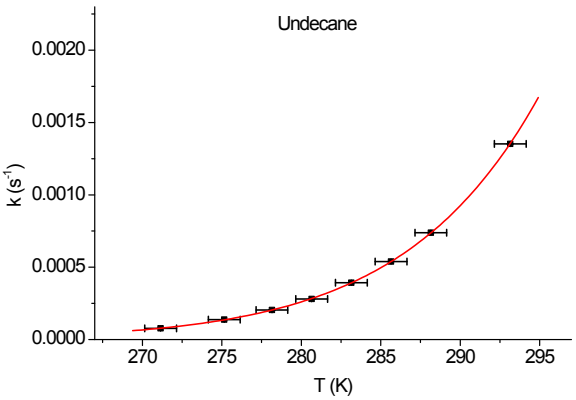
Undecane
k (s-1)
T (K)

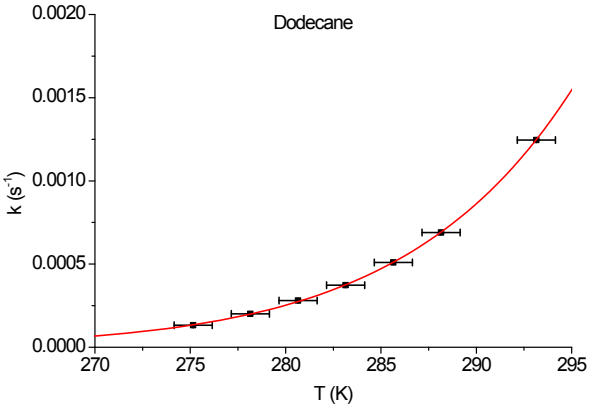
Dodecane
k (s-1)
T (K)

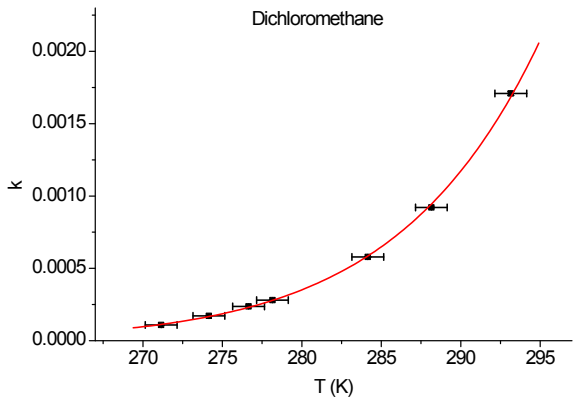
Dichloromethane
k
T (K)

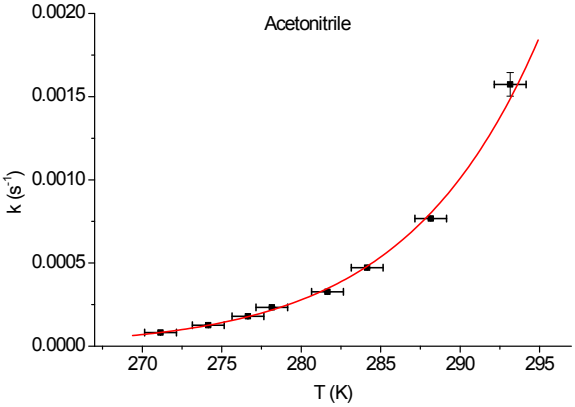
Acetonitrile
k (s-1)
T (K)

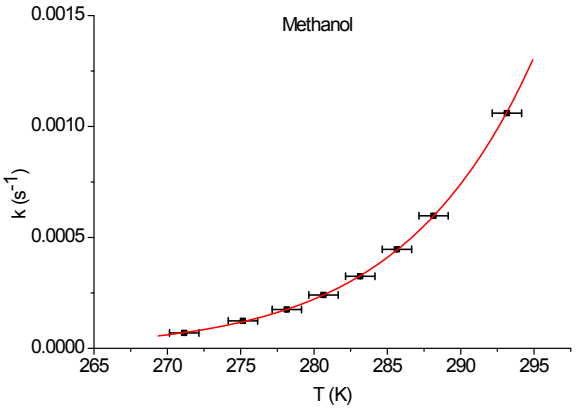
Methanol
k (s-1)
T (K)

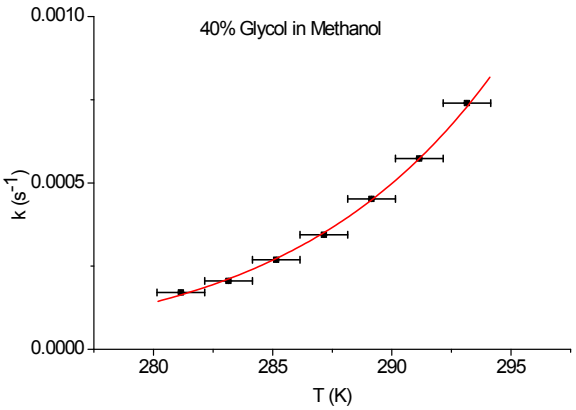
40% Glycol in Methanol
k (s-1)
T (K)

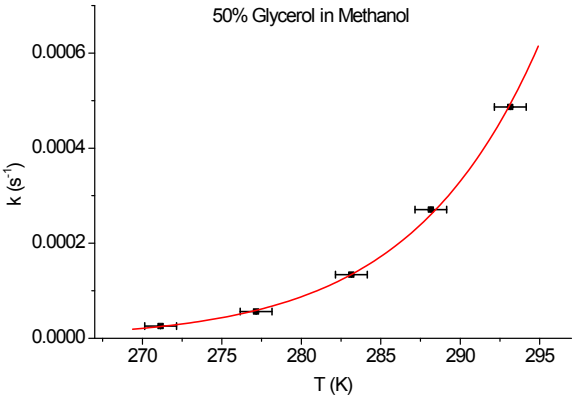
50% Glycerol in Methanol
k (s-1)
T (K)

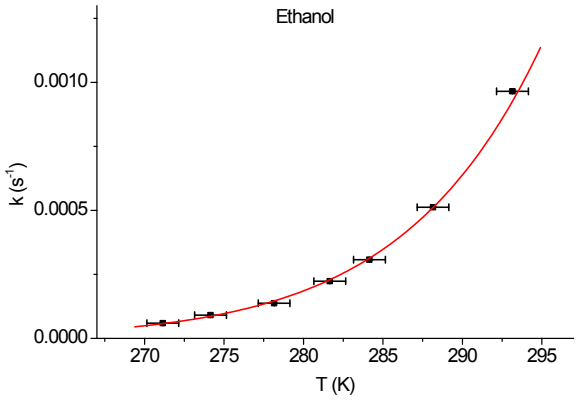
Ethanol
k (s-1)
T (K)

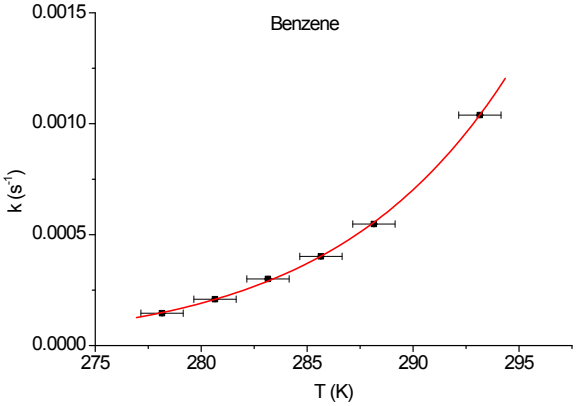
Benzene
k (s-1)
T (K)

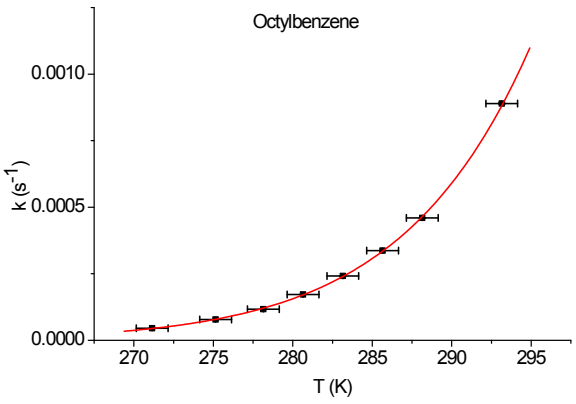
Octylbenzene
k (s-1)
T (K)

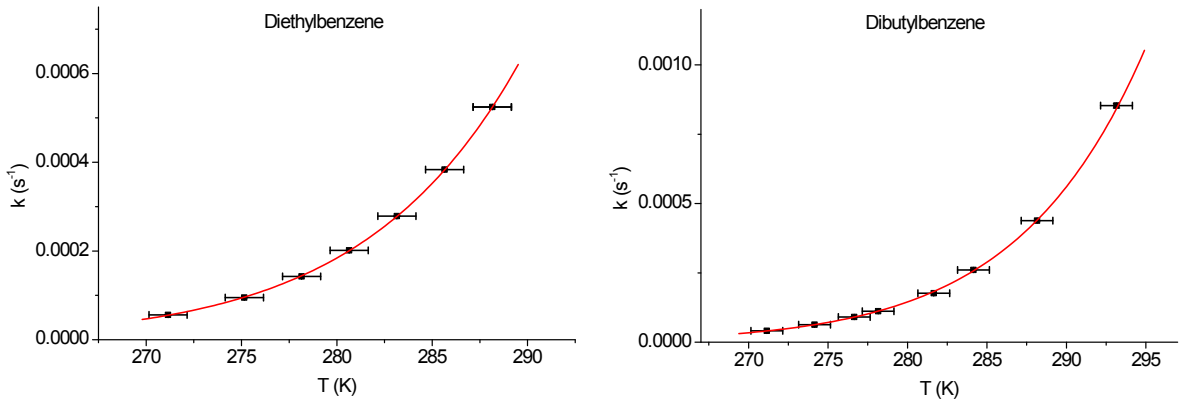

Figure 4: Eyring plots for several solvents. Eyring plots for pentane, hexane, heptane, octane, nonane, decane and dodecane have been published previously.

Table 4: Activation parameters for the 17 solvents at 20 ºC and ambient pressure.

Solvent	$t_{1/2}$ (min)	$\Delta^{\ddagger}H^{o}$ (kJ mol^{-1})	$\Delta^{\ddagger}S^{o}$ (J K^{-1} mol^{-1})	$\Delta^{\ddagger}G^{o}$ (kJ mol^{-1})
Pentane	5.52±0.14	74.0±1.3	-43.6±4.7	86.8±0.1
Hexane	5.80±0.17	76.0±1.5	-37.4±5.2	86.9±0.1
Heptane	6.28±0.17	80.4±1.5	-22.9±5.2	87.1±0.1
Octane	6.87±0.18	76.0±1.4	-38.8±4.9	87.3±0.1
Nonane	7.33±0.20	80.3±1.5	-24.6±5.1	87.5±0.1
Decane	7.80±0.22	82.7±1.5	-17.0±5.3	87.6±0.1
Undecane	8.52±0.24	83.3±1.5	-15.6±5.4	87.9±0.1
Dodecane	9.25±0.27	80.6±1.8	-25.6±6.4	88.0±0.1
Dichloromethane	6.77±0.19	79.0±1.4	-28.5±4.9	87.3±0.1
Acetonitrile	7.72±0.24	84.6±1.5	-10.5±5.4	87.6±0.1
Methanol	10.9±0.29	79.1±1.4	-32.0±5.1	88.4±0.1
50% Glycerol in methanol	23.3±0.76	87.4±1.7	-9.90±6.1	90.3±0.1
40% Glycol in methanol	15.9±0.43	83.0±2.7	-21.7±9.3	89.4±0.1
Ethanol	12.4±0.35	81.1±1.5	-26.4±5.2	88.8±0.1
Benzene	11.1±0.37	85.6±2.4	-9.94±8.5	88.5±0.1
Octylbenzene	13.1±0.39	87.5±1.6	-4.88±5.6	88.9±0.1
Diethylbenzene	12.0±0.48	83.7±2.0	-17.0±7.0	88.7±0.1
Dibutylbenzene	13.7±0.43	88.8±1.5	-0.676±5.5	89.0±0.1

3. Fatigue test

A $2 \cdot 10^{-5}$ M solution of motor **1** was prepared in heptane and purged with argon. The sample was subjected to 8 continuous rotation cycles at 15 °C and the UV absorption was monitored at 410 nm. The photoisomerization was performed by irradiating the sample for 45 min with 365 nm light. Subsequently the sample was left in the dark for 1 h. Figure 5 shows the absorptions at 410 nm for 8 isomerization cycles, demonstrating that motor **1** shows excellent fatigue resistance.

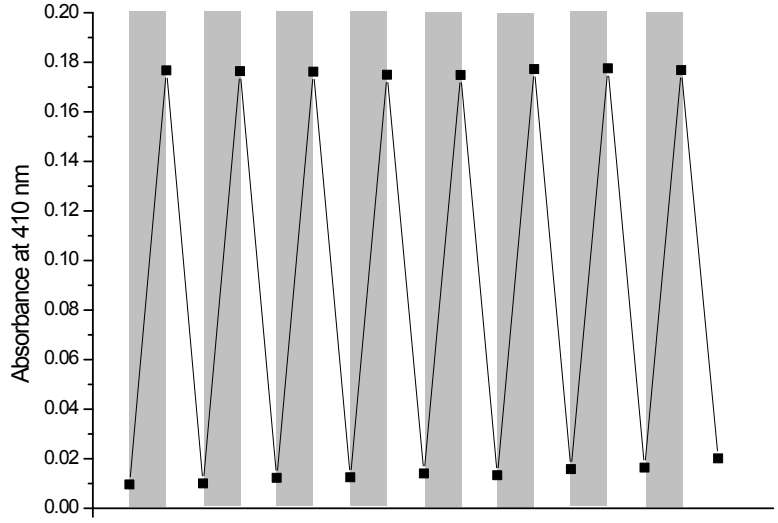

Figure 5: Fatigue test for motor **1**. Irradiation with 365 nm light (grey areas) was followed by leaving the sample in the dark (white areas).

4. Viscosity measurements

The kinematic viscosity of the solvents used was measured in triplo using an Ubbelohde viscometer (type I, 0 or 0c). The viscometer was placed in a water bath with temperature probe to ensure constant temperature and prevent fluctuations. Solvent was run 3x through the viscometer before measurement. The density of the solvents was determined by weighing 10 mL of solvent in a volumetric flask, and the dynamic viscosity was calculated from the 2 obtained values.

5. Statistical Analysis

The coefficient of determination (R^2) was calculated for all specific solvent groups for the linear relationship of ln η vs ln k (Table 5). To determine the linearity of this relationship the Pearson product-moment correlation coefficient (Pearson's r) was calculated and reported with its probability (p-value). The sign indicates the direction of the trend, zero signifies complete randomness and |1| signifies a perfect linear relationship. Pearson's r values ≥ |0.708| mean that more than 50% of the variance is related, Pearson's r values ≥ |0.995| mean that more than 99% of the variance is related; p-values < 0.01 indicate a significant relationship.[4]

Table 5: Statistical results of ln η vs ln k for specific solvent groups. Significant linear relationships are bold.

Solvent group	Symbol	R^2	Pearson's r	p-value
Alkanes	■	0.994	-0.997	**0.000**
Methanol/Glycerol	▲	0.998	-0.999	**0.000**
Methanol/Glycol/Glycerol	▲✕	0.987	-0.993	**0.000**
Linear Alcohols	◆	0.412	-0.642	0.062
Mono-aromatics	■	0.922	-0.960	**0.001**
Bis-aromatics	●	0.972	-0.986	0.014
Cycloalkanes	◆	0.930	-0.965	0.035

The Pearson's r is appropriate to evaluate the relationship between ln k and ln η since it is expected to be linear. For the relationships of other solvent properties with ln k it is not required of them to be linear. The Spearman's ρ is an ideal statistical tool to identify the presence and strength of a monotonic relationship in a dataset (a monotonic function is one that either never increases or never decreases as its independent variable increases).[4–6] For completeness both statistical parameters were determined with their corresponding probability (Table 6). The sign indicates the direction of the trend, zero signifies complete randomness and |1| signifies a perfect linear or monotonic relationship and p-values < 0.01 indicate a significant relationship. For significant correlations, one might wish to label the strength of the association, however, the limits chosen for this are often arbitrary and based on the context of the study.[4] We prefer to be strict in the assignment of association strength, and we label any association which explains less then 1/3 of the variance ($\rho < |0.58|$) as weak, up to 1/2 of the variance ($|0.58| \leq \rho < |0.71|$) as moderate, up to 2/3 of the variance ($|0.71| \leq \rho < |0.82|$) as strong and more than 2/3 ($\rho \geq |0.82|$) as very strong.

Table 6: Statistical results of various solvent properties vs ln k. Strong correlations as well as significant relationships are bold.

Property	Pearson's r	p-value	Spearman's ρ	p-value
ln η	-0.689	**0.000**	**-0.728**	**0.000**
π*	-0.445	0.043	-0.345	0.126
ε	-0.322	0.155	-0.571	**0.007**
$E_T(30)$	-0.585	**0.004**	-0.629	**0.002**
α	-0.509	0.016	-0.411	0.057
β	-0.640	**0.001**	-0.703	**0.000**
ST	-0.460	**0.009**	-0.437	0.014
D	**0.774**	**0.002**	**0.797**	**0.001**
c.e.d.	-0.632	**0.004**	**-0.782**	**0.000**

As discussed in the main text, three solvent properties display a significant strong correlation (ln η, c.e.d. and D). It is interesting to note that the only strong linear relationship is that of diffusion. It is, however, unfair to compare these results directly to oneanother, since the datasets differ from each other (see main

text, Table 2). To allow for a fair comparison of the correlation of a solvent property (x) with the natural log of the rate (ln k) and the correlation of the natural log of viscosity (ln η) with the natural log of the rate (ln k), the data missing from solvent property 'x' was also removed from the 'ln η' dataset, after which the correlations coefficients were calculated again (Table 7). The correlation coeffecients for the solvent property 'x' naturally remain unchanged with respect to Table 6, as well as their respective p-values which are not shown in Table 7. For the modified 'ln η' datasets, all p-values for both correlation coefficients are < 0.01 with one exception ($p = 0.012$ for Pearson's r of ln η vs ln k for property 'D'). The comparison shows that for both the linear as well as the monotonic relationships ln η scores higher than the other solvent properties with the notable exception of the diffusion (D). Not only does the monotonic relationship between the diffusion and the natural log of the rate score higher, so does too the linear relationship. This is discussed in the main text.

Table 7: Statistical results of various solvent properties vs ln *k* with modified datasets for ln *η*.

Property (x)	Pearson's r of x vs ln k	Pearson's r of ln η vs ln k	Spearman's ρ of x vs ln k	Spearman's ρ of ln η vs ln k	R^2 improvement ratio
π*	-0.445	-0.655	-0.345	-0.742	1.22
ε	-0.322	-0.683	-0.571	-0.774	1.05
ET(30)	-0.585	-0.686	-0.629	-0.781	1.11
α	-0.509	-0.662	-0.411	-0.748	1.03
β	-0.640	-0.662	-0.703	-0.748	1.08
ST	-0.460	-0.654	-0.437	-0.711	1.13
D	0.774	-0.674	0.797	-0.764	1.37
c.e.d.	-0.632	-0.749	-0.782	-0.809	1.43

One of the goals was to explain the differences found between certain solvent groups for the viscosity dependence of the rate for THI. This explanation was sought after in the presented solvent properties, i.e. if for example in a certain solvent property the alcohol and aromatic values are grouped separately from the aliphatics, it might provide a reason for the observed difference in viscosity dependence. Since such an explanation was not visually apparent, an attempt was made to provide a quantitized comparison.

The desired 'correction' factor sought after in the additional solvent properties should increase the linearity of the ln η vs ln k relationship. This is expressed in the Pearson's r, though with the data randomly distributed over ln η it is equally well expressed in the coefficient of determination, R^2. The same datasets were used as for the correlation coefficients comparison in Table 7. Each set of ln η vs ln k was fitted against eq. 4 (*vide supra*) by least squares which provided their respective R^2's. Subsequently the solvent property data was added to each corresponding dataset and using least squares were fitted against eq. 8:

$$\ln k = \beta - \alpha \cdot \ln \eta + \gamma \cdot x. \qquad (8)$$

in which γ is a correction factor similar to α and x is the corresponding solvent property. There are nearly infinite other possible functions to which ln η and x vs ln k can be fitted using three variables (α, β and γ), however, with the limited available data this would prove to be a fruitless exercise since any random dataset of comparable size would be provided with a reasonable fit. Therefore we are only interested in the known linear relationship between ln η and ln k on which we investigate a linear correction for x. The least squares analysis provides improved coefficients of determination for (ln η and x vs ln k), which is appropriately compared as the ratio of $(1-R^2_{\ln \eta})/(1- R^2_{x, \ln \eta})$ (Table 7). This is to be expected from the addition of $\gamma \cdot x$ since any dataset which deviates from perfect randomness would positively contribute to such a regression. Therefore it is important to evaluate to which extent the correlation has improved after the addition of $\gamma \cdot x$ and to determine whether it is significant. To determine what constitutes a significant improvement of $(1-R^2_{\ln \eta})/(1- R^2_{x, \ln \eta})$, a Monte Carlo analysis is performed which revealed that for these datasets the improvement has to be ≥1.45 in order to fall outside of 99% random improvement (p-value < 0.01). The only solvent property which comes close to such an improvement is the cohesive energy density,

which already exhibits a reasonably strong correlation by itself. Therefore, from this analysis no additional information could be obtained regarding the differences in the solvent groups with respect to the viscosity dependence of their rates.

6. References

(1) Kistemaker, J. C. M.; Lubbe, A. S.; Bloemsma, E. A.; Feringa, B. L. *Chem. Phys. Chem.* **2016**, *asap*.

(2) Gegiou, D.; Muszkat, K. A.; Fischer, E. *J. Am. Chem. Soc.* **1968**, *90*, 12–18.

(3) Liu, L.; Guo, Q.-X. *Chem. Rev.* **2001**, *101*, 673–696.

(4) Campbell, M. J.; Swinscow, T. D. V. *Statistics at Square One*, 11th ed.; Wiley-Blackwell, 2009.

(5) Spearman, C. *Am. J. Psychol.* **1904**, *15*, 72–101.

(6) Corder, G. W.; Foreman, D. I. *Nonparametric Statistics for Non-Statisticians*; John Wiley & Sons, Inc.: Hoboken, NJ, USA, 2009.

7. General Methods

Chemical were purchased from Sigma Aldrich, Acros or TCI Europe N.V.; solvent were reagent grade and distilled and dried before use according to standard procedures, if required. Column chromatography was performed on silica gel (Silica Flash P60, 230–400 mesh). ^{1}H and ^{13}C-NMR were recorded on a Varian Gemini-200 (50 MHz), or a Varian AMX400 (101 MHz). DOSY-NMR was recorded on a Varian **XX**. Chemical shifts are denoted in δ values (ppm) relative to $CDCl_3$ (^{1}H: δ = 7.26 and ^{13}C: δ = 77.16). For ^{1}H-NMR, the splitting parameters are designated as follows: s (singlet), d (doublet), t (triplet), q (quartet), p (pentet), h (heptet), m (multiplet) and app (apparent). HRMS spectra were recorded on a Thermo Fischer Scientific Orbitrap XL with ESI and/or APCI ionization sources. UV-vis absorption spectra were measured on a Jasco V-630 spectrometer. Irradiation was performed using a Spectroline ENB-280C/FE lamp (365 nm).

8. Experimental Procedures

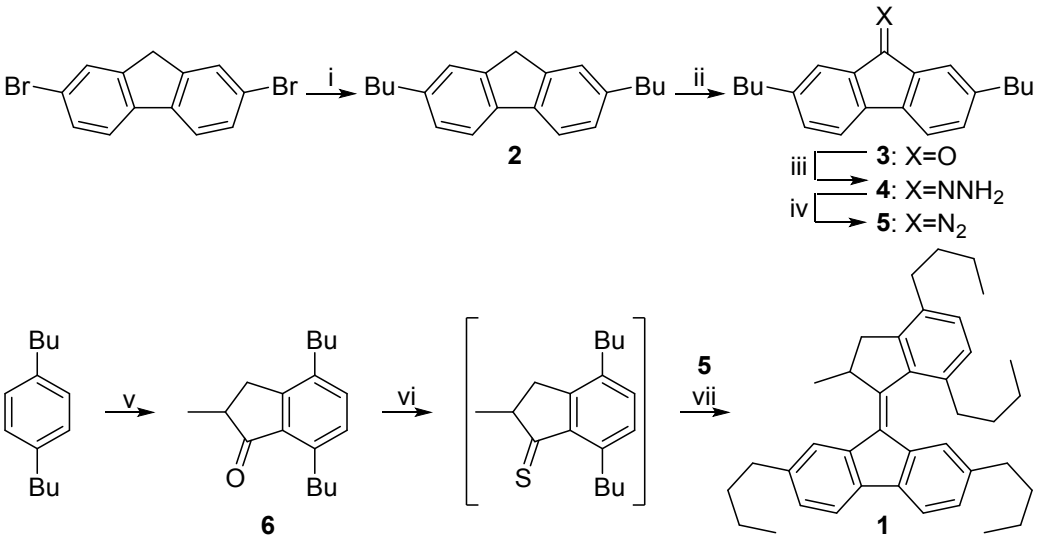

i) 2.4 eq BuLi, 1 mol% $Pd(PtBu_3)_2$, toluene, 49%; ii) Triton B, air, pyridine, 12 h, 73%; iii) $N_2H_4 \cdot H_2O$, MeOH, 16 h, 95%; iv) MnO_2, THF, 66%; v) $AlCl_3$, DCM, methacrylic acid, −75 °C to reflux, 2 h, 31%; vi) P_4S_{10}, Lawesson's reagent, toluene, 60 °C to reflux, 16 h; vii) **5**, toluene, THF, 40 °C, 16 h, 60% over 2 steps, 1.47 g of **1**.

Figure 6: Synthesis of molecular motor **1**.

The synthesis of molecular motor **1** has been previsously described and is shown in Figure 6.[1] Motor **1** was obtained as a yellow liquid. ^{1}H NMR (400 MHz, Chloroform-*d*) δ 7.69 (d, *J* = 1.4 Hz, 1H), 7.66 (d, *J* = 7.7 Hz, 1H), 7.59 (d, *J* = 7.7 Hz, 1H), 7.36 (s, 1H), 7.18 (dd, *J* = 7.9, 1.0 Hz, 1H), 7.14 (s, 1H), 7.08 (dd, *J* = 7.7, 0.8 Hz, 1H), 4.15 (app. p, *J* = 6.6 Hz, 1H), 3.21 (dd, *J* = 14.8, 5.9 Hz, 1H), 2.83 (dt, *J* = 14.0, 8.0 Hz, 1H), 2.76 (t, *J* = 7.7 Hz, 2H), 2.66 (app. dt, *J* = 14.2, 7.6 Hz, 1H), 2.63 (d, *J* = 14.8 Hz, 1H), 2.61 (app. dt, *J* = 14.2, 7.8 Hz, 1H), 2.58 (app. dt, *J* = 14.1, 7.0 Hz, 1H), 2.51 (t, *J* = 7.6 Hz, 2H), 1.72 (app. p, *J* = 7.6 Hz, 2H), 1.63 (app. p, *J* = 7.6 Hz, 2H), 1.55 (app. p, *J* = 7.5 Hz, 2H), 1.46 (app. h, *J* = 7.4 Hz, 2H), 1.42 (app. h, *J* = 7.4 Hz, 2H), 1.39 (app. p, *J* = 7.6 Hz, 3H), 1.35 (d, *J* = 6.9 Hz, 2H), 1.32 (app. h, *J* = 7.4 Hz, 2H), 1.01 (app. h, *J* = 7.1 Hz, 2H), 1.00 (t, *J* = 7.4 Hz, 3H), 0.97 (t, *J* = 7.4 Hz, 3H), 0.91 (t, *J* = 7.4 Hz, 3H), 0.67 (t, *J* = 7.4 Hz, 3H). ^{13}C NMR (101 MHz, Chloroform-*d*) δ 152.08 (C), 144.33 (C), 141.18 (C), 140.81 (C), 140.17 (C), 139.96 (C), 139.61 (C), 138.33 (C), 137.99 (C), 137.32 (C), 136.63 (C), 130.08 (C), 129.47 (CH), 127.60 (CH), 127.48 (CH), 127.16 (CH), 124.19 (CH), 123.50 (CH), 119.14 (CH), 118.59 (CH), 44.14 (CH), 39.75 (CH_2), 36.38 (CH_2), 35.94 (CH_2), 34.32 (CH_2), 34.10 (CH_2), 34.05 (CH_2), 33.62 (CH_2), 32.73 (CH_2), 32.55 (CH_2), 22.81 (CH_2), 22.56 (CH_2), 22.43 (CH_2), 22.07 (CH_2), 19.19 (CH_3), 14.21 (CH_3), 14.18 (CH_3), 14.15 (CH_3), 14.03 (CH_3). HRMS (ESI-pos): calcd for ($[C_{39}H_{50} + H]^+$) 519.3985, found 519.3973.

The photochemical properties of motor **1** were previously studied via UV-vis and NMR spectroscopy.[1] It was shown that upon irradiation with 365 nm light, the stable-**1** isomerizes to metastable-**1** (^{1}H-NMR: stable/metastable 24:76 in CD_2Cl_2).The stable form can be completely regenerated by heating.

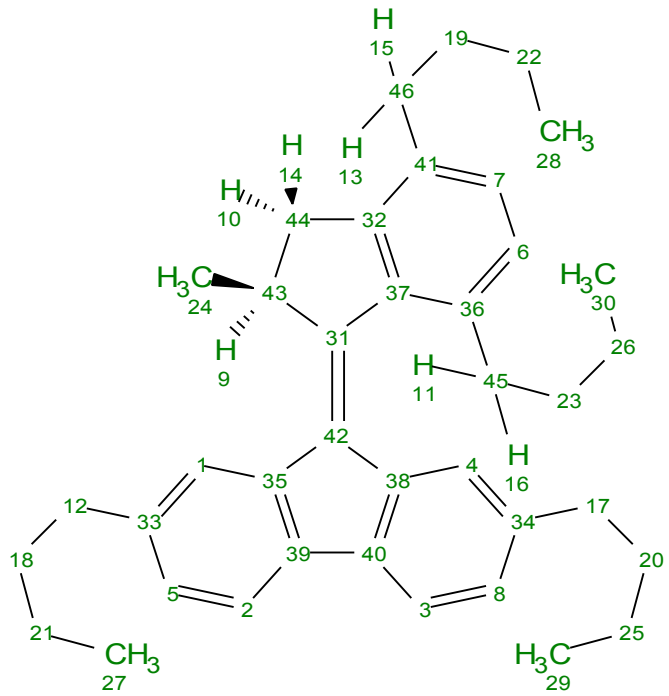

NOESY: protons 1→9,12,24; 4→11,16,17.